Biogeosciences Discuss., 9, 7197–7226, 2012
www.biogeosciences-discuss.net/9/7197/2012/
doi:10.5194/bgd-9-7197-2012

Biogeosciences Discussions

Ocean acidification mediates photosynthetic response to UV radiation and temperature increase in the diatom *Phaeodactylum tricornutum*

Y. Li[1], K. Gao[1], V. E. Villafañe[2], and E. W. Helbling[2]

[1]State Key Laboratory of Marine Environmental Science, Xiamen University, Xiamen, 361005, China
[2]Estación de Fotobiología Playa Unión and Consejo Nacional de Investigaciones Científicas y Técnicas (CONICET) Casilla de Correos No. 15 (9103) Rawson, Chubut, Argentina

Received: 1 June 2012 – Accepted: 5 June 2012 – Published: 18 June 2012

Correspondence to: K. Gao (ksgao@xmu.edu.cn)

Published by Copernicus Publications on behalf of the European Geosciences Union.

Abstract

Increasing atmospheric CO_2 concentration is responsible for progressive ocean acidification, ocean warming as well as decreased thickness of upper mixing layer (UML), thus exposing phytoplankton cells not only to lower pH and higher temperatures but also to higher levels of solar UV radiation. In order to evaluate the combined effects of ocean acidification, UV radiation and temperature, we used the diatom *Phaeodactylum tricornutum* as a model organism and examined its physiological performance after grown under two CO_2 concentrations (390 and 1000 µatm) for more than 20 generations. Compared to the ambient CO_2 level (390 µatm), growth at the elevated CO_2 concentration increased non-photochemical quenching (NPQ) of cells and partially counteracted the harm to PSII caused by UV-A and UV-B. Such an effect was less pronounced under increased temperature levels. As for photosynthetic carbon fixation, the rate increased with increasing temperature from 15 to 25 °C, regardless of their growth CO_2 levels. In addition, UV-induced inhibition of photosynthesis was inversely correlated to temperature. The ratio of repair to UV-induced damage showed inverse relationship with increased NPQ, showing higher values under the ocean acidification condition against UV-B, reflecting that the increased pCO_2 and lowered pH counteracted UV-B induced harm.

1 Introduction

The increase in atmospheric CO_2 concentration is expected to influence the acid-base balance in the pelagic (McNeil and Matear, 2008) as well as in the coastal waters (Cai et al., 2011) due to increasingly dissolved CO_2, leading to ocean acidification (Sabine et al., 2004). By the end of this century, atmospheric CO_2 levels are expected to increase to 800–1000 ppmv (IPCC A1F1 scenario) while surface seawater pH would be reduced by 0.3–0.4 pH units (100–150 % increase in H^+ concentration) (Caldeira and Wickett, 2003; Orr et al., 2005). Ocean acidification is known to reduce calcification

BGD
9, 7197–7226, 2012

of coccolithophores (Beaufort et al., 2011; Riebesell and Tortell, 2011) and coralline algae (Gao et al., 1993; Gao and Zheng, 2010). On the one hand, increasing pCO_2 in seawater has been shown to stimulate growth and photosynthetic carbon fixation rates of phytoplankton (Hein and Sand-Jensen, 1997; Schippers et al., 2004; Riebesell et al., 2007; Wu et al., 2010; McCarthy et al., 2012), while neutral effects of CO_2 enrichment were also reported (Tortell et al., 2000; Tortell and Morel, 2002; Fu et al., 2007). On the other hand, the increase in pCO_2 may alter phytoplankton community structure (Tortell et al., 2002), and enhance mitochondria respiration (Wu et al., 2010). Ocean acidification is not an isolated process and thus interactive effects with other climate changes, like increasing temperature and UV radiation (UVR, 280–400 nm), needs to be considered in an holistic way (Boyd, 2011; Hutchins, 2011).

With increasing atmospheric CO_2 concentration, global temperature is expected to increase by 2.5–6.4 °C in the atmosphere (Alexiadis, 2007) and by 2–3 °C in the surface oceans by the yr 2100 (Houghton et al., 2001). Such changes will also have important effects on various organisms, since most physiological processes are temperature-dependent (Allakhverdiev et al., 2008). It is known that temperature affects the morphology (Mühling et al., 2003) and biochemical composition (Mühling et al., 2005) of cyanobacteria. However, differential responses to the combined "greenhouse" (warming as well as elevated CO_2) treatment have been found in the marine picocyanobacteria *Synechococcus* and *Prochlorococcus*, with the growth rate of the former increasing and that of the latter not changing (Fu et al., 2007). Hutchins (2007) reported that either elevated CO_2 (750 ppmv) or a 4 °C temperature increase stimulated the growth and nitrogen fixation rate of the filamentous cyanobacterium *Trichodesmium* sp., however, synergistic effects among these two variables had not been observed. A 5 °C temperature rise only increased photosynthesis and calcification of *Emiliania huxleyi* grown under Ca^{2+} sufficient but not under Ca^{2+} deficient conditions (Xu et al., 2011). Nevertheless, the "greenhouse" increased the coccolithophore cell abundance (Feng et al., 2009). The distributions and ecological niches of major phytoplankton groups like dinoflagellates (Peperzak, 2003; Cloern et al., 2005; Hallegraeff, 2010), diatoms,

BGD
9, 7197–7226, 2012

and coccolithophores (Merico et al., 2004; Hare et al., 2007) have been suggested to change with ocean warming. The acceleration of the spring phytoplankton bloom and changes in dominant species were affected by the combination of warming and high light levels (Lewandowska and Sommer, 2010). It is known that a "stratified greenhouse" of the surface oceans has been affected by progressive oceanic warming and acidification (Doney, 2006; Beardall et al., 2009), therefore, phytoplankton cells will be exposed to "greenhouse" under increasing exposures to solar visible and ultraviolet radiation (UVR, 280–400 nm).

Solar UV-B (280–315 nm) radiation at the Earth's surface has been shown to increase due to the ozone depletion and its interplay with climate change (Manney et al., 2011). UVR (UV-A+UV-B) is known to inhibit growth and photosynthesis (Helbling et al., 1992; Heraud and Beardall, 2000; Gao et al., 2007a; Jiang and Qiu, 2011) and damage proteins and the DNA molecule (Grzymski et al., 2001; Xiong, 2001; Gao et al., 2008). However, moderate UVR levels were shown to increase photosynthetic carbon fixation (Nilawati et al., 1997; Barbieri et al., 2002), with UV-A (320–400 nm) even driving photosynthetic carbon fixation in the absence of PAR (Gao et al., 2007b).

In an ecological context, where organisms are exposed to the influence of several abiotic and biotic factors, the effects of multiple factors can greatly differ from simple combinations of single-factor responses (Christensen et al., 2006), i.e. variables can act in synergistic or antagonistic ways (Dunne, 2010). For example, at ambient CO_2 level, the presence of UVR stimulated calcification of *E. huxleyii* (Guan and Gao, 2010), however, at elevated CO_2 levels, it inhibited calcification (Gao et al., 2009). Fu (2008) reported that only simultaneous increases in both CO_2 and temperature enhanced the maximum light-saturated carbon fixation rate (P_{Bmax}) of the raphidophyte *Heterosigma akashiwo*, whereas CO_2 enrichment with or without increased temperature had effects on P_{Bmax} (with increased or reduced P_{Bmax} under high CO_2 or high temperature treatment, respectively) of the dinoflagellate *Prorocentrum minimum*. Under ocean acidification conditions, UV-B inhibited growth of the red tide alga *Phaeocystis globosa* (Chen and Gao, 2011).

BGD
9, 7197–7226, 2012

Obviously, more attention is being paid to the study of the interactive effects of multiple stressors and ocean acidification on different taxonomic groups; however, diatoms have surprisingly received less attention. Changes in seawater carbonate system, such as increased pCO_2 and HCO_3^- concentrations and decreased pH, may affect phytoplankton's energetics to maintain their intracellular acid-base stability and thus their physiology to cope with additional environmental changes. Consequently, we hypothesize that diatoms grown under ocean acidification condition (high CO_2/lower pH) will be more sensitive to increases of UVR and temperature than cells grown at ambient CO_2 level. To test this hypothesis we chose the cosmopolitan diatom species *Phaeodactylum tricornutum* as model organism, and the process studied was photosynthesis, via carbon incorporation and photochemical measurements.

2 Materials and methods

2.1 Organism model and culture conditions

Phaeodactylum tricornutum Bohlin (strain CCMA 106, isolated from the South China Sea (SCS) in 2004) was obtained from the Center for Collections of Marine Bacteria and Phytoplankton (CCMBP) of the State Key Laboratory of Marine Environmental Science, Xiamen University. Cultures were grown in 0.22 µm filtered natural seawater collected from the South China Sea (SEATS station: 116° E, 18° N) and enriched with Aquil medium (Morel et al., 1979). The cultures were maintained at 20 °C for about 20 generations before used in experiments. During this period, cultures were illuminated with cool white fluorescent tubes that provided 70 µmol photons m^{-2} s^{-1} of Photosynthetic Active Radiation (PAR; 12L:12D). The cultures were continuously aerated (350 ml min^{-1}), with ambient CO_2 level (LC, 390 µatm) or CO_2 enriched (HC, 1000 µatm) air which was controlled with a CO_2 plant chamber (HP1000G-D, Wuhan Ruihua Instrument and Equipment Co., Ltd., Wuhan, China) with variations <4 %.

BGD
9, 7197–7226, 2012

Semi-continuous cultures were operated by diluting them with the CO_2-equilibrated media every 24 h, and the cell's concentrations were maintained within a range of 7×10^4–3×10^5 cells ml^{-1}, so that the seawater carbonate system parameters were stable (Table 1) with pH variations <0.02 units. Cell concentrations were determined using a Coulter Counter (Z-2, Beckman) before and after the dilution (prior to the start of dark period); pH was measured with a pH meter (Benchtop pH 510, OAKTON) that was calibrated daily with a standard National Bureau of Standards (NBS) buffer (Hanna). Other parameters of the seawater carbonate system (Table 1) were calculated using the CO2SYS software (Lewis and Wallace, 1998) taking into account the salinity, pCO_2, pH, nutrient concentrations and temperature; the equilibrium constants K_1 and K_2 for carbonic acid dissociation and K_B for boric acid were determined according to Roy et al. (1993) and Diskson (1990), respectively.

2.2 Experimental set up

Samples of *P. tricornutum* (either from LC or HC) were harvested (concentration of ~2×10^5 cells ml^{-1}), resuspended in fresh medium to a final concentration of ~2×10^4 cells ml^{-1} and put either in 35 or 100 ml quartz tubes (for carbon uptake or measurements of fluorescence parameters, respectively, see below). Three radiation treatments were implemented (with triplicate samples for each treatment): (1) PAB (PAR+UV-A+UV-B) treatment: quartz tubes covered with Ultraphan film 295 (Digefra, Munich, Germany), thus receiving irradiances above 295 nm; (2) PA (PAR+UV-A) treatment: quartz tubes covered with Folex 320 film (Montagefolie, Folex, Dreieich, Germany), samples receiving irradiances above 320 nm; and (3) P treatment: quartz tubes covered with Ultraphan film 395 (UV Opak, Digefra), samples receiving only PAR (400–700 nm). The transmission of these cut-off foils and quartz tubes are available elsewhere (Figueroa et al., 1997). The tubes for carbon incorporation and for fluorescence measurements were placed under a solar simulator (Sol 1200W; Dr. Hönle, Martinsried, Germany). The cells were exposed to irradiances of 63.5 W m^{-2} (PAR, 290 µmol photons m^{-2} s^{-1}), 23.1 W m^{-2} (UV-A) and 1.20 W m^{-2} (UV-B) for 60 min under

BGD
9, 7197–7226, 2012

three temperature levels: 15, 20 and 25 °C, by maintaing the tubes in a circulating water bath for temperature control (CTP-3000, Eyela). During the exposures, measurements of fluorescence parameters were done (see below); after exposure, part of the samples were processed for carbon uptake measurements, while part of them were allowed to recover for 80 min (under the initial growth light level), during which fluorescence parameters were measured (see below).

2.3 Measurements and analysis

2.3.1 Radiation measurements

The irradiances received by the cells were measured using a broad-band filter radiometer (ELDONET, Real Time Computer, Möhrendorf, Germany) that has channels for UV-B (280–315 nm), UV-A (315–400 nm) and PAR (400–700 nm).

2.3.2 Effective photochemical quantum yield

For the determination of the effective photochemical quantum yield (Φ_{psII}), aliquots of 2 ml of sample from each tube (total of 9 tubes i.e. triplicate per each treatment) were taken every 1 min, both during exposure and recovery, and immediately measured (without any dark adaptation) using a xenon – pulse amplitude modulated fluorometer (XE-PAM, Walz, Germany). Each sample was measured 4 times and the Φ_{psII} was determined by measuring the instant maximum fluorescence (F'_m) and the steady state fluorescence (F_t) of the light-adapted cells and calculated according to Genty et al. (1989) as: $\Phi_{psII} = (F'_m - F_t)/F'_m = \Delta F/F'_m$. Non-photochemical quenching (NPQ) was calculated as: $NPQ = (F_m - F'_m)/F'_m$, where F_m represents the maximum fluorescence yield after dark adaptation for 10 min and F'_m the maximum fluorescence yield determined using a saturating white light pulse (5000 µmol photons m^{-2} s^{-1} in 0.8 s) at the actinic light levels (300 µmol photons m^{-2} s^{-1}, similar to the exposure PAR level).

BGD
9, 7197–7226, 2012

The inhibition of Φ_{psII} due to UVR, UV-A, or UV-B was calculated as:

$$Inh_{UVR}(\%) = (\Phi_{psIIP} - \Phi_{psIIPAB})/(\Phi_{psIIP}) \times 100 \quad (R1)$$

$$Inh_{UV\text{-}A}(\%) = (\Phi_{psIIP} - \Phi_{psIIPA})/(\Phi_{psIIP}) \times 100 \quad (R2)$$

$$Inh_{UV\text{-}B}(\%) = (\Phi_{psIIPA} - \Phi_{psIIPAB})/(\Phi_{psIIP}) \times 100 = Inh_{UVR}(\%) - Inh_{UV\text{-}A}(\%) \quad (R3)$$

where Φ_{psIIP}, Φ_{psIIPA}, and $\Phi_{psIIPAB}$ indicate the values of Φ_{psII} in the P, PA and PAB treatments, respectively.

The rates of UV-induced damage to the photosynthetic apparatus (k, in min^{-1}) and repair (r, in min^{-1}) were estimated according to Heraud and Beardall (2000).

2.3.3 Photosynthetic carbon uptake

Samples were inoculated with 5 µCi (0.185 MBq) of labeled sodium bicarbonate (ICN Radiochemicals). A total of 20 tubes (6 for each radiation treatment, plus 2 dark controls) were exposed under the solar simulator, with 3 tubes per radiation treatment (plus 2 dark) being filtered (Whatman GF/F, 25 mm) right after the 60 min of the exposures, while the other 9 tubes were filtered after the 60 min of recovery. After filtration, the filters were placed into 20 ml scintillation vials, exposed to HCl fumes overnight in darkness, and dried at 45 °C for 4 h. Scintillation cocktail (Wallac Optiphase Hisafe 3, Perkin Elmer Life and Analytical Sciences, USA) was added to the vials, and the samples were counted after 1 h using a liquid scintillation counter (LS6500 Multi-Purpose Scintillation Counter, Bechman Counter, USA). The rate of photosynthetic carbon fixation was calculated according to Holm-Hansen and Helbling (1995). The inhibition due to UVR, UV-A or UV-B was determined in the same way as described for Φ_{psII}.

2.3.4 Chlorophyll *a* (chl *a*)

Concentration of chl *a* at the beginning of the exposures was determined by filtering ~250 ml of culture onto a Whatman GF/F filter (diameter: 25 mm), extracted in 5 ml

BGD
9, 7197–7226, 2012

absolute methanol overnight at 4 °C, and then centrifuged (10 min at 5000 g). The absorption spectrum of the supernatant was obtained by scanning the sample from 250 to 750 nm with a scanning spectrophotometer (DU 800, Beckman Coulter Inc.) and the concentration of chl *a* was calculated using the equation of Porra (2002).

2.3.5 Data analysis

Three replicates for each radiation/temperature/CO_2 conditions were used in all experiments, so that the data is plotted as mean and standard deviation values. Three- and two ways ANOVA tests were used to determine the interaction between UVR, temperature and CO_2 concentration, or among two of these variables, respectively. The two-sample paired t-test was also used to determine significant differences between CO_2, temperature or UV treatments. Significant level was set at $P < 0.05$.

3 Results

3.1 Carbonate system during semi-continuous growth

The pH levels in the LC or HC cultures were 8.16 (±0.01) and 7.82 (±0.02), respectively, being significantly different ($P < 0.01$, two samples paired t-test). In the HC cultures, DIC, HCO_3^- and CO_2 levels were significantly higher by 11.8 %, 16.9 % and 156.3 %, respectively, and that of CO_3^{2-} was lower by 46.6 %. There was no significant difference in the total alkalinity between the two cultures, with the variations being <0.4 %.

3.2 Photochemical responses

The effective photochemical quantum yield (Φ_{psII}) of *P. tricornutum* decreased significantly during the first 10–20 min of exposure in all (radiation/temperature/CO_2) treatments (Fig. 1); after this period, Φ_{psII} remained more or less constant. These

BGD
9, 7197–7226, 2012

trends were best described and fitted using a first order exponential decrease function ($\Phi_{psII} = a + b^{*}e^{(-c^{*}t)}$; t represents the time of exposure; (a), (b) and (c) are adjustment parameters). Regardless of the temperature and CO_2 levels, the samples receiving PAR alone had less decrease in Φ_{psII} (i.e. the lowest value reached ca. 0.5) after 10–20 min of exposure than those additionally receiving UV-A (in which Φ_{psII} decreased to 0.3–0.4) or UV-A+B (Φ_{psII} decreased to 0.2–0.3). At the same temperature level, HC-grown cells had generally better photochemical performance (i.e. higher Φ_{psII}) than LC-grown ones, and this was more evident in the UVR-treated samples. These differences in photochemical responses were clearly seen when plotting the Φ_{psII} ratios of HC- to LC-grown cells (Fig. 2), which was ~1 in the P treatment at all temperatures. In the presence of UV-A or UV-A+UV-B, these trends were of increasing HC/LC Φ_{psII} ratio during the 10–20 min of exposure, and then leveling off and maintaining rather constant values. The ratios HC/LC Φ_{psII}, however, increased with increasing temperature, for example, under the PAB treatment, the ratios had mean values of 1.22, 1.30, and 1.41 for samples exposed at 15, 20 and 25 °C, respectively. At 25 °C, samples receiving UV-B had a significant higher ($P < 0.01$) HC/LC Φ_{psII} ratio than samples in the PA treatment; however, no significant differences were found between the PA and PAB treatments at 15 or 20 °C ($P > 0.1$).

In order to determine the potential "protecting" role of excess energy dissipation via non-photochemical quenching (NPQ), the variations of the ratio of repair (r) to damage (k) – r/k–, estimated from the changes in Φ_{psII} over time were plotted against NPQ (Fig. 3). Inverse linear relationships were observed, with high r/k-values associated with lower NPQ ones. Under the PA treatment, r/k in LC and HC-grown cells had a similar decrease with increasing NPQ values (Fig. 3a). The addition of UV-B reduced r/k significantly ($P < 0.05$) (Fig. 3b) and lead to a differential decrease of the ratio between the HC and LC-grown cells. Nevertheless, HC-grown cells always had higher r/k than LC-grown cells at all NPQ values.

Once the stress was removed (i.e. after exposure, when the samples were shifted to low light levels), Φ_{psII} recovered; this recovery was best described and fitted by

BGD
9, 7197–7226, 2012

a first order exponential equation: $\Phi_{psII} = a + b^* (1 - e^{(-c^* t)})$ (t represents the time of exposure; (a), (b) and (c) are rate constants) (Fig. 4). Pre-exposure to UV-A and UV-B markedly hindered the recovery of Φ_{psII}, especially in the 15 °C treatment for the LC-grown cells (Fig. 4a). However, the recovery rate of the LC-grown cells increased with temperature (Figs. 4a, c and e). In the HC-acclimated cells (Figs. 4b, d and f), the differences in recovery among the radiation treatments were not significant regardless of the preceding exposures to UVR with the exception of that incubated at 15 °C under the PAB treatment ($P < 0.05$). Within the same experimental temperature level, HC-grown cells had in general higher recovery rates than LC-grown ones, especially in cells that received UVR.

3.3 Photosynthetic carbon fixation responses

Chl *a* content did not change throughout the exposure period within each CO_2 treatment and there was no significant difference in the chl *a* content between the LC- and HC-grown cells (i.e. 0.27 vs. 0.26 pg chl *a* cell^{-1}, with standard division <0.017 for triplicate cultures).

The photosynthetic carbon fixation rates during the exposures and recovery are shown in Fig. 5. After 60 min of exposure (Fig. 5a, c and e), the LC-grown cells had higher photosynthetic carbon fixation rates than the HC-grown ones, with the highest values found under the P treatment at 25 °C (~1.36 pg C cell^{-1} h^{-1}). Moreover, the presence of UV-A or UV-A+UV-B reduced photosynthetic carbon fixation regardless of the growth CO_2 conditions or temperature levels. Increasing temperature from 15 °C (Fig. 5a) to 20 or 25 °C (Fig. 5c and e) significantly enhanced carbon fixation rates ($P < 0.01$). During the next 60 min recovery period, no significant differences among radiation treatments in the LC-grown cells were found at 15 or 25 °C (Fig. 5b, f) but at 20 °C, carbon fixation was lower in the PAB than under the P or PA treatments (Fig. 5d). The HC-grown cells, instead, presented different responses: The lowest values were determined at 15 °C (Fig. 5b) whereas the highest were determined at 20 °C (Fig. 5d).

BGD
9, 7197–7226, 2012

When comparing photosynthetic carbon fixation rates among the exposure and recovery periods, it was seen that they were in general significantly higher ($P < 0.05$) when UV-A or UV-A+B was removed during recovery period, except that at 25 °C. At 20 °C, the carbon fixation rate was higher ($P < 0.01$) under the low PAR received during the recovery period, regardless the CO_2 levels.

When the UVR-induced inhibition of the photosynthetic carbon fixation was compared among the different treatments (Fig. 6) it was seen that UV-A induced the highest inhibition at the lower temperature (15 °C) (Fig. 6a). The HC-grown cells showed higher sensitivity to UV-B at the lower temperature, but a reversed trend was observed at higher temperatures (20 and 25 °C), although the differences were not significant ($P > 0.1$). The "greenhouse" effects significantly reduced the photosynthetic inhibition ($P < 0.05$) caused by both UV-A (Fig. 6a) and UV-B (Fig. 6b).

4 Discussion

Global climate change brings about a combination of several factors that act together in such a way that they modify the dynamics of the ocean systems and hence, of the communities living there. In our study, we addressed the combined effects of three variables associated to climate change, i.e. ocean acidification (as addressed by rise in CO_2 and H^+ concentrations), UVR and temperature on the cosmopolitan diatom *Phaeodactylum tricornutum*. Overall, we determined that the "greenhouse" treatment resulted in a generally better photosynthetic performance of this species and less sensitivity to UVR.

When exposed to solar radiation in the presence of UVR, the HC-grown cells had a better photochemical performance (i.e. less decrease of Φ_{psII}) than those grown at LC conditions (Fig. 1d, f). However, the LC-grown cells had slightly higher photosynthetic carbon fixation rates than the HC-grown ones (Fig. 5), though mostly insignificant except under the P or PA treatments at 15 and 20 °C. It has been previously found that effects of climate change variables were different according to the photosynthetic targets

BGD
9, 7197–7226, 2012

examined (Helbling et al., 2011), which could explain at least part of the differences observed between LC and HC pre-acclimated cells. Moreover, Wu et al. (2010) found for *P. tricornutum* that respiration was enhanced in the HC-grown cells and that its carbon concentration mechanisms (CCMs) were down-regulated. Photorespiration was also higher in the HC-grown cells of this species (Gao et al., 2012). On the other hand, high contribution of net CO_2 uptake (about two-thirds) to total inorganic carbon acquisition was reported in *P. tricornutum* (Burkhardt et al., 2001; Hopkinson et al., 2011). Together with the down-regulation of CCM (meaning a lowered active uptake of inorganic carbon), enhancement of mitochondrial- and photo-respiration could have led to decreased photosynthetic carbon fixation due to the additional carbon losses. The stimulated quantum yield in the HC-cells appeared to be attributed to the extra carbon loss, i.e. extra electron drainage.

The UVR-induced inhibition of the effective photochemical quantum yield was inversely correlated with temperature (Fig. 3). At the low temperature, the LC-grown cells showed higher UVR-induced inhibition of photochemical efficiency (Fig. 1) and the recovery was slower (Fig. 4) compared with the HC-grown ones. The "greenhouse" treatment resulted in a significant ($P < 0.05$) decrease of UV-induced inhibition from 50–60 % to 27–36 %, of which UV-B accounted for about 8 % and 14 %, respectively. And this trend appears to be similar to the changes observed in photosynthetic carbon fixation, as increase in its rates with increasing temperature was higher in the HC than in the LC-grown cells (Fig. 5a, c and e), reflecting a synergistic effect of pCO_2 rise and warming. This might be associated with enhanced activity of cellular enzymes and membrane fluidity, as they are temperature-dependent (Allakhverdiev et al., 2008), and accelerated molecular repair rates that usually increase with temperature within a species' thermal window (Conkling and Drake, 1984; Gao et al., 2008). In the presence of UV-B, NPQ in the LC-grown cells was lower than HC-grown ones, especially under the lower temperature treatment (Fig. 3b). Down-regulation of CCM might have aided to enhance NPQ in the HC-grown cells due to the saved energy demand for CO_2 active uptake, which could lead to an additional light stress (Gao et al., 2012).

BGD
9, 7197–7226, 2012

Activity and gene expression of Rubisco in the diatom *Thalassiossira weissflogii* increased with increased temperature, and this might have partially counteracted the UVR-induced inhibition of photosynthetic carbon fixation (Helbling et al., 2011). On the other hand, high levels of UVR can lead to degradation of periplasmic carbonic anhydrase (CAe) (Wu and Gao, 2009) as well as Rubisco and D1 protein (Bischof et al., 2002; Bouchard et al., 2005), and increased temperature could have stimulated the repair of the damaged molecules. The beneficial effects of increased temperature on photosynthesis under UVR stress have been previously documented (Sobrino and Neale, 2007; Gao et al., 2008; Halac et al., 2010; Helbling et al., 2011), showing lower UVR-induced inhibition or damages at higher temperatures. Differential sensitivities to UVR have been reported in marine picoplankters when grown under elevated CO_2 concentrations, with *Nannochloropsis gaditana* having lower sensitivity while *Nannochloris atomus* showed neutral response (Sobrino et al., 2005). For the diatom *Thalassiosira pseudonana*, when grown at elevated CO_2 concentration, it became more sensitive to UVR (Sobrino et al., 2008). In the present study, when the photosynthetic carbon fixation and Φ_{psII} were compared, the UVR-induced inhibition was lower on the former than on the latter, and higher CO_2 weakened this inhibition. Regardless of the pre-acclimation CO_2 levels, less inhibition caused by UVR on the carbon fixation might be due to stimulation of the activity of CAe (Wu and Gao, 2009) which catalyzes the interconversion of bicarbonate and CO_2, therefore, stimulating the uptake of CO_2 during the exposures. Additionally, the increase of r/k with temperature was higher in the HC than in the LC-grown cells, which reflects enhanced repair in these cells, as UVR-induced molecular damage was independent of temperature (Ishigaki et al., 1999).

In terms of ecological implications, future "greenhouse" ocean with decreased thickness of the upper mixing layer (enhanced stratification) may expose phytoplankton cells to higher exposure to solar UVR as well as PAR. For diatoms like *P. tricornutum*, increased CO_2 and seawater acidity might counteract somehow the harm caused by UV-B. Since UV-A results in negative effects under high but positive ones under reduced levels of solar radiation on phytoplankton carbon fixation, playing a double-edged

BGD
9, 7197–7226, 2012

effects on phytoplankton (Gao et al., 2007b), its simulative effects would be enlarged under ocean acidification conditions (Chen and Gao, 2011). Thus, the net effects of UVR, temperature and CO_2 will largely depend on the levels of solar radiation to which the phytoplankton cells are exposed. Consequently, mixing rates or mixing depth will explicitly affect the combined effects of the above climate change variables, as mixing expose cells to fluctuating irradiances which can affect the balance between photodamage and repair of PSII. Increased NPQ, as found in this study, closely related to the decreases (UVR-related) of the ratio between damage and repair rate (r/k) of PSII in *P. tricornutum*. The increased seawater acidity must have stimulated photoprotective processes, thus, leading to higher NPQ, which was especially pronounced in the presence of UV-B (Fig. 3). Increasing temperature, in some cold or temperate waters, may help the species like *P. tricornutum* to counteract negative effects of UVR or ocean acidification-induced harm. On the other hand, diversified responses to combined effects of climate change variables are expected in view of their diversities in physiological pathways and ecological niches.

Acknowledgements. This study was supported by National Basic Research Program of China (No. 2009CB421207 and 2011CB200902), Program for Changjiang Scholars and Innovative Research Team (IRT0941), National Natural Science Foundation (No. 40930846, No. 41120164007) and China-Japan collaboration project from MOST (S2012GR0290), and Consejo Nacional de Investigaciones Científicas y Técnicas – Argentina (PIP 12-201001-00228). VEV and EWH were supported by the Visiting Professor Program (111) from the Ministry of Education of China. This is Contribution No. 127 of Estación de Fotobiología Playa Unión.

References

Alexiadis, A.: Global warming and human activity: A model for studying the potential instability of the carbon dioxide/temperature feedback mechanism, Ecol. Model., 203, 243–256, doi:10.1016/j.ecolmodel.2006.11.020, 2007.

BGD
9, 7197–7226, 2012

Allakhverdiev, S., Kreslavski, V. D., Klimov, V. V., Los, D. A., Carpentier, R., and Mohanty, P.: Heat stress: an overview of molecular responses in photosynthesis, Photosynth. Res., 98, 541–550, doi:10.1007/s11120-008-9331-0, 2008.

Barbieri, E. S., Villafañe, V. E., and Helbling, E. W.: Experimental assessment of UV effects on temperate marine phytoplankton when exposed to variable radiation regimes, Limnol. Oceanogr., 47, 1648–1655, 2002.

Beaufort, L., Probert, I., de Garidel-Thoron, T., Bendif, E. M., Ruiz-Pino, D., Metzl, N., Goyet, C., Buchet, N., Coupel, P., Grelaud, M., Rost, B., Rickaby, R. E. M., and de Vargas, C.: Sensitivity of coccolithophores to carbonate chemistry and ocean acidification, Nature, 476, 80–83, doi:10.1038/nature10295, 2011.

Beardall, J., Sobrino, C., and Stojkovic, S.: Interactions between the impacts of ultraviolet radiation, elevated CO_2, and nutrient limitation on marine primary producers, Photochem. Photobio. S., 8, 1257–1265, doi:10.1039/b9pp00034h, 2009.

Bischof, K., Kräbs, G., Wiencke, C., and Hanelt, D.: Solar ultraviolet radiation affects the activity of ribulose-1, 5-bisphosphate carboxylase-oxygenase and the composition of photosynthetic and xanthophyll cycle pigments in the intertidal green alga *Ulva lactuca* L., Planta, 215, 502–509, doi:10.1007/s00425-002-0774-9, 2002.

Bouchard, J. N., Campbell, D. A., and Roy, S.: Effects of UV-B radiation on the D1 protein repair cycle of natural phytoplankton communities from three latitudes (Canada, Brazil, and Argentina), J. Phycol., 41, 273–286, 2005.

Bowler, C., Allen, A. E., Badger, J. H., Grimwood, J., Jabbari, K., Kuo, A., Maheswari, U., Martens, C., Maumus, F., Otillar, R. P., Rayko, E., Salamov, A., Vandepoele, K., Beszteri, B., Gruber, A., Heijde, M., Katinka, M., Mock, T., Valentin, K., Verret, F., Berges, J. A., Brownlee, C., Cadoret, J.-P., Chiovitti, A., Choi, C. J., Coesel, S., De Martino, A., Detter, J. C., Durkin, C., Falciatore, A., Fournet, J., Haruta, M., Huysman, M. J. J., Jenkins, B. D., Jiroutova, K., Jorgensen, R. E., Joubert, Y., Kaplan, A., Kröger, N., Kroth, P. G., La Roche, J., Lindquist, E., Lommer, M., Martin-Jézéquel, V., Lopez, P. J., Lucas, S., Mangogna, M., McGinnis, K., Medlin, L. K., Montsant, A., Oudot-Le Secq, M.-P., Napoli, C., Obornik, M., Parker, M. S., Petit, J.-L., Porcel, B. M., Poulsen, N., Robison, M., Rychlewski, L., Rynearson, T. A., Schmutz, J., Shapiro, H., Siaut, M., Stanley, M., Sussman, M. R., Taylor, A. R., Vardi, A., von Dassow, P., Vyverman, W., Willis, A., Wyrwicz, L. S., Rokhsar, D. S. Weissenbach, J., Armbrust, E. V., Green, B. R., Van de Peer, Y., and Grigoriev, I. V.: The *Phaeodactylum* genome reveals the

BGD
9, 7197–7226, 2012

evolutionary history of diatom genomes, Nature, 456, 239–244, doi:10.1038/nature07410, 2008.
Boyd, P. W.: Beyond ocean acidification, Nat. Geosci., 4, 273–274, doi:10.1038/ngeo1150, 2011.
Burkhardt, S., Amoroso, G., Riebesell, U., and Sültermeyer, D.: CO_2 and HCO_3^- uptake in marine diatoms acclimated to different CO_2 concentrations, Limnol. Oceanogr., 46, 1378–1391, 2001.
Cai, W.-J., Hu, X. P., Huang, W.-J., Murrell, M. C., Lehrter, J. C., Lohrenz, S. E., Chou, W.-C., Zhai, W. D., Hollibaugh, J. T., Wang, Y. C., Zhao, P. S., Guo, X. H., Gundersen, K., Dai, M. H., and Gong, G.-C.: Acidification of subsurface coastal waters enhanced by eutrophication, Nat. Geosci., 4, 766–770, doi:10.1038/NGEO1297, 2011.
Caldeira, K. and Wickett, M. E.: Anthropogenic carbon and ocean pH, Nature, 425, p. 365, 2003.
Chen, S. W. and Gao, K. S.: Solar ultraviolet radiation and CO_2-induced ocean acidification interacts to influence the photosynthetic performance of the red tide alga *Phaeocystis globosa* (Prymnesiophyceae), Hydrobiologia, 675, 105–117, doi:10.1007/s10750-011-0807-0, 2011.
Christensen, M. R., Graham, M. D., Vinebrooke, R. D., Findlay, D. L., Paterson, M. J., and Turner, M. A.: Multiple anthropogenic stressors cause ecological surprises in boreal lakes, Global Change Biol., 12, 2316–2322, doi:10.1111/j.1365-2486.2006.01257.x, 2006.
Cloern, J. E., Schraga, T. S., Lopez, C. B., Knowles, N., Labisoa, R. G., and Dugdale, R.: Climate anomalies generate an exceptional dinoflagellate bloom in San Francisco Bay, Geophys. Res. Lett., 32, L14608, doi:10.1029/2005GL023321, 2005.
Conkling, M. A. and Drake, J. W.: Thermal rescue of UV-irradiated bacteriophage T4 and biphasic mode of action of the WXY system, Genetics, 107, 525–536, 1984.
Dickson, A. G.: Standard potential of the reaction: AgCl(s) + $^1/_2$ H_2(g) = Ag(s) + HCl(aq), and the standard acidity constant of the ion HSO_4^- in synthetic seawater from 273.15 to 318.15 K, J. Chem. Thermodyn., 22, 113–127, 1990.
Doney, S. C.: The dangers of ocean acidification, Sci. Am., 294, 58–65, 2006.
Dunne, R. P.: Synergy or antagonism – interactions between stressors on coral reefs, Coral Reefs, 29, 145–152, doi:10.1007/s00338-009-0569-6, 2010.
Feng, Y. Y., Hare, C. E., Leblanc, K., Rose, J. M., Zhang Y. H., DiTullio, G. R., Lee, P. A., Wilhelm, S. W., Rowe, J. M., Sun, J., Nemcek, N., Gueguen, C., Passow, U., Benner, I., Brown, C., and Hutchins, D. A.: Effects of increased PCO_2 and temperature on the North

BGD
9, 7197–7226, 2012

Atlantic spring bloom. I., The phytoplankton community and biogeochemical response, Mar. Ecol.-Prog. Ser., 388, 13–25, doi:10.3354/meps08133, 2009.
Figueroa, F. L., Salles, S., Aguilera, J., Jiménez, C., Mercado, J., Viinegla, B., FloresMoya, A., Altamirano, M.: Effects of solar radiation on photoinhibition and pigmentation in the red *Porphyra leucosticta*, Mar. Ecol.-Prog. Ser., 151, 81–90, 1997.
Fu, F. X., Mark, E. W., Zhang Y. H., Feng Y. Y., and Hutchins, D. A.: Effects of increased temperature and CO_2 on photosynthesis, growth, and elemental ratios in marine *Synechococcus* and *Prochlorococcus* (Cyanobacteria), J. Phycol., 43, 485–496, doi:10.1111/j.1529-8817.2007.00355.x, 2007.
Fu, F. X., Zhang, Y. H., Warner, M. E., Feng, Y. Y., and Huntchins, D. A.: A comparison of future increased CO_2 and temperature effects on sympatric *Heterosigma akashiwo* and *Prorocentrum minimum*, Harmful Algae, 7, 76–90, doi:10.1016/j.hal.2007.05.006, 2008.
Gao, K. S., Aruga, Y., Asada, K., Ishihara, T., Akano, T., and Kiyohara, M.: Calcification in the areticulated coralline algal *Corallina pilulifera*, with special referance to the effect of elevated CO_2 concentration, Mar. Biol., 117, 129–132, 1993.
Gao, K. S., Guan, W. C., and Helbling, E. W.: Effects of solar ultraviolet radiation on photosynthesis of the marine red tide alga *Heterosigma akashiwo* (Raphidophyceae), J. Photoch. Photobio. B., 86, 140–148, doi:10.1016/j.jphotobiol.2006.05.007, 2007a.
Gao, K. S., Li, P., Walanabe, T., and Helbling, E. W.: Combined effects of ultraviolet radiation and temperature on morphology, photosynthesis, and DNA of *Arthrospira (Spirulina) platensis*(Cyanophyta), J. Phycol., 44, 777–786, doi:10.1111/j.1529-8817.2008.00512.x, 2008.
Gao, K. S., Wu, Y. P., Li, G., Wu, H. Y., Villafañe, V. E., and Helbling, E. W.: Solar UV radiation drives CO_2 fixation in marine phytoplankton: A double-edged sword, Plant Physiol., 144, 54–59, doi:10.1104/pp.107.098491, 2007b.
Gao, K. S., Xu, J. T., Gao, G., Li, Y. H., Hutchins, D. A., Huang, B. Q., Wang, L., Zheng, Y., Jin, P., Cai, X. N., Häder, D.-P., Li, W., Xu, K., Liu, N. N., and Riebesell, U.: Rising CO_2 and increased light exposure synergistically reduce marine primary productivity, Nature Climate Change, doi:10.1038/NCLIMATE1507, in press, 2012.
Gao, K. S. and Zheng, Y. Q.: Combined effects of ocean acidification and solar UV radiation on photosynthesis, growth, pigmentation and calcification of the coralline alga *Corallina sessilis* (Rhodophyta), Glob. Change Biol., 16, 2388–2398, doi:10.1111/j.1365-2486.2009.02113.x, 2010.

BGD
9, 7197–7226, 2012

Genty, B. E., Briantais, J. M., and Baker, N. R.: Relative quantum ef?ciencies of the two photosystems of leaves in photorespiratory and non-photorespiratory conditions, Plant Physiol. Biochem., 28, 1–10, 1989.

Grzymski, J., Orrico, C., and Schofield, O. M.: Monochromatic ultraviolet light induced damage to Photosystem II efficiency and carbon fixation in the marine diatom *Thalassiosira pseudonana* (3H), Photosynth. Res., 68, 181–192, 2001.

Guan, W. C. and Gao, K. S.: Impacts of UV radiation on photosynthesis and growth of coccolithophore *Emiliania huxleyi* (Haptophyceae), Environ. Exp. Bot., 67, 502–508, doi:10.1016/j.envexpbot.2009.08.003, 2010.

Halac, S. R., Villafañe, V. E., and Helbling, E. W.: Temperature benefits the photosynthetic performance of the diatoms *Chaetoceros gracilis* and *Thalassiosira weissflogii* when exposed to UVR, J. Photoch. Photobio. B., 101, 196–205, doi:10.1016/j.jphotobiol.2010.07.003, 2010.

Hallegraeff, G. M.: Ocean climate change, phytoplankton community responses, and harmful algal blooms: a formidable predictive challenge, J. Phycol., 46, 220–235, doi:10.1111/j.1529-8817.2010.00815.x, 2010.

Hare, C. E., Leblanc, K., Ditullio, G. R., Kudela, R. M., Zhang, Y. H., Lee, P. A., Riseman, S., and Hutchins, D. A.: Consequences of increased temperature and CO_2 for phytoplankton community structure in the Bering Sea, Mar. Ecol.-Prog. Ser., 352, 9–16, doi:10.3354/meps07182, 2007.

Hein, M. and Sand-Jensen, K.: CO_2 increases oceanic primary production, Nature, 388, 526–527, 1997.

Helbling, E. W., Buma, A. G. J., Boelen, P., van der Strate, H. J., Fiorda Giordanino, M. V, and Villafañe, V. E.: Increase in Rubisco activity and gene expression due to elevated temperature partially counteracts ultraviolet radiation–induced photoinhibition in the marine diatom *Thalassiosira weissflogii*, Limnol. Oceanogr., 56, 1330–1342, doi:10.4319/lo.2011.56.4.1330, 2011.

Helbling, E. W., Villafañe, V. E., Ferrario, M. E., and Hansen, O. H.: Impact of natural ultraviolet radiation on rates of photosynthesis and on specific marine phytoplankton species, Mar. Ecol.-Prog. Ser., 80, 89–100, 1992.

Heraud, P., and Beardall, J.: Changes in chlorophyll fluorescence during exposure of *Dunaliella tertiolecta* to UV radiation indicate a dynamic interaction between damage and repair processes, Photosynth. Res., 63, 123–134, 2000.

BGD
9, 7197–7226, 2012

Holm-Hansen, O. and Helbling, E. W.: Técnicas para la medición de la productividad primaria en el fitoplancton, in: Manual de Métodos Ficológicos, edited by: Alveal, K., Ferrario, M. E., Oliveira, E. C., and Sar, E., Universidad de Concepción, Concepción, Chile, 329–350, 1995.

Hopkinson, B. M., Dupont, C. L., Allen, A. E., and Morel, F. M. M.: Efficiency of the CO_2-concentrating mechanism of diatom, P. Natl. Acad. Sci. USA, 108, 3830–3837, doi:10.1073/pnas.1018062108, 2011.

Houghton, J. T., Ding, Y., Griggs, D. J., Noguer, M., Van Der Linden, P. J., Dai, X., Mashell, L., and Johnson, C. A.: Climate change 2001: the scientific basis, Cambridge University Press, Cambridge, 2001.

Hutchins, D. A.: Oceanography: Forecasting the rain ratio, Nature, 476, 41–42, doi:10.1038/476041a, 2011.

Hutchins, D. A., Fu, F. X., Zhang, Y. H., Warner, M. E., Feng, Y. Y., Portune, K., Bernhardt, P. W., and Mulholland, M. R.: CO_2 control of *Trichodesmium* N_2 fixation, photosynthesis, growth rates, and elemental ratios: Implications for past, present, and future ocean biogeochemistry, Limnol. Oceanogr., 52, 1293–1304, 2007.

Ishigaki, Y., Takayama, A., Yamashita, S., and Nikaido, O.: Development and characterization of a DNA solar dosimeter, J. Photoch. Photobio. B, 50, 184–188, 1999.

Jiang, H. B. and Qiu, B. S.: Inhibition of photosynthesis by UV-B exposure and its repair in the bloom-forming cyanobacterium *Microcystis aeruginosa*, J. Appl. Phycol., 23, 691–696, doi:10.1007/s10811-010-9562-2, 2011.

Lesser, M. P., Cullen, J. J., and Neale, P. J.: Carbon uptake in a marine diatom during acute exposure to ultraviolet B radiation: Relative importance of damage and repair, J. Phycol., 30, 183–192, 1994.

Lewandowska, A. and Sommer, U.: Climate change and the spring bloom: a mesocosm study on the influence of light and temperature on phytoplankton and mesozooplankton, Mar. Ecol.-Prog. Ser., 405, 101–111, doi:10.3354/meps08520, 2010.

Lewis, E. and Wallace, D. W. R.: Program Developed for CO_2 System Calculations, ORNL/CDIAC-105, Carbon Dioxide Information Analysis Center, Oak Ridge National Laboratory, US Department of Energy, 1998.

Manney, G. L., Santee, M. L., Rex, M., Livesey, N. J., Pitts, M. C., Veefkind, P., Nash, E. R., Wohitmann, I., Lehmann, R., Froidevaux, L., Poole, L. R., Schoeberl, M. R., Haffner, D. P., Davies, J., Dorokhov, V., Gernandt, H., Johnson, B., Kivi, R., Kyrö, E., Larsen, N., Levelt, P. F., Makshtas, A., McElroy, T., Nakajima, H., Parrondo, M. C., Tarasick, D. W., von der Gathen,

BGD
9, 7197–7226, 2012

P., Walker, K. A., and Zinoviev, N. S.: Unprecedented Arctic ozone loss in 2011, Nature, 478, 469–475, doi:10.1038/nature10556, 2011.
McCarthy, A., Rogers, S. P., Duffy, S. J., and Campbell, D. A.: Elevated carbon dioxide differentially alters the photophysiology of *Thalassiosira pseudonana* (Bacillariophyceae) and *Emiliania huxlieyi* (Haptophyta), J. Phycol., 47, doi:10.1111/j.1529-8817.2012.01171.x, in press, 2012.
McNeil, B. I. and Matear, R. J.: Southern Ocean acidification: A tipping point at 450-ppm atmospheric CO_2, P. Natl. Acad. Sci. USA, 105, 18860–18864, 2008.
Merico, A., Tyrrell, T., Lessard, E. J., Oguz, T., Stabeno, P. J., Zeeman, S. I., and Whitledge, T. E.: Modelling phytoplankton succession on the Bering Sea shelf: role of climate influences and trophic interactions in generating *Emiliania huxleyi* blooms 1997–2000, Deep-Sea Res., 51, 1803–1826, doi:10.1016/j.dsr.2004.07.003, 2004.
Morel, F. M. M., Rueter, J. G., Anderson, D. M., and Guillard, R. R. L.: Aquil: A chemically defined phytoplankton culture medium for trace metal studies, J. Phycol., 15, 135–141, 1979.
Mühling, M., Belay, A., and Whitton, B. A.: Variation in fatty acid composition of *Arthrospira* (Spirulina) strains, J. Appl. Phycol., 17, 137–146, doi:10.1007/s10811-005-7213-9, 2005.
Mühling, M., Harris, N., Belay, A., and Whitton, B. A.: Reversal of helix orientation in the cyanobacterium *Arthrospira*, J. Phycol., 39, 360–367, 2003.
Nilawati, J., Greenberg, B. M., and Smith, R. E. H.: Influence of ultraviolet radiation on growth and photosynthesis of two cold ocean diatoms, J. Phycol., 33, 215–224, 1997.
Orr, J. C., Fabry, V. J., Aumont, O., Bopp, L., Doney, S. C., Feely, R. A., Gnanadesikan, A., Gruber, N., Ishida, A., Joos, F., Key, R. M., Lindsay, K., Maier-Reimer, E., Matear, R., Monfray, P., Mouchet, A., Najjar, R. G., Plattner, G. K., Rodgers, K. B., Sabine, C. L., Sarmiento, J. L., Schlitzer, R., Slater, R. D., Totterdell, I. J., Weirig, M. F., Yamanaka, Y., and Yool, A.: Anthropogenic ocean acidification over the twenty-first century and its impact on calcifying organisms, Nature, 437, 681–686, 2005.
Peperzak, L.: Climate change and harmful algal blooms in the North Sea, Acta Oecol., 24, S139–S144, 2003.
Porra, R. J.: The chequered history of the development and use of simultaneous equations for the accurate determination of chlorophylls a and b, Photosynth. Res., 73, 149–156, 2002.
Riebesell, U., Schulz, K. G., Bellerby, R. G. J., and Botros, M.: Enhanced biological carbon consumption in a high CO_2 ocean, Nature, 450, 545–548, doi:10.1038/nature06267, 2007.

BGD
9, 7197–7226, 2012

Riebesell, U. and Tortell, P. D.: Effects of ocean acidification on pelagic organisms and ecosystems, in: Ocean acidification, edited by: Gattuso, J.-P., and Hansson, L.: Oxford University Press, UK, 99–116, 2011.

Roy, R. N., Roy, L. N., Vogel, K. M., Porter-Moore, C., Pearson, T., Good, C. E., Millero, F. J., and Campbell, D. M.: The dissociation constants of carbonic acid in seawater at salinities 5 to 45 and temperature 0 to 45°C, Mar. Chem., 44, 249–267, 1993.

Sabine, L. C., Feely, R. A., Gruber, N., Key, R. M., Lee, K., Bullister, J. L., Wanninkhof, R., Wong, C. S., Wallace, D. W. R., Tilbrook, B., Millero, F. J., Peng, T.-H., Kozyr, A., Tsueno, O., and Rios, A. F.: The oceanic sink for anthropogenic CO_2, Science, 305, 367–371, doi:10.1126/science.1097403, 2004.

Schippers, P., Lurling, M., and Scheffer, M.: Increase of atmospheric CO_2 promotes phytoplankton productivity, Ecol. Lett., 7, 446–451, doi:10.1111/j.1461-0248.2004.00597.x, 2004.

Sobrino, C. and Neale, P. J.: Short-term and long-term effects of temperature on photosynthesis in the diatom *Thalassiosira pseudonana* under UVR exposures, J. Phycol., 43, 426–436, doi:10.1111/j.1529-8817.2007.00344.x, 2007.

Sobrino, C., Neale, P. J., and Lubian, L. M.: Interaction of UV radiation and inorganic carbon supply in the inhibition of photosynthesis: Spectral and temporal responses of two marine picoplankters, Photochem. Photobiol., 81, 384–393, 2005.

Sobrino, C., Ward, M. L., and Neale, P. J.: Acclimation to elevated carbon dioxide and ultraviolet radiation in the diatom *Thalassiosira pseudonana*: Effects on growth, photosynthesis, and spectral sensitivity of photoinhibition, Limnol. Oceanogr., 53, 494–505, 2008.

Tortell, P. D., Ditullio, G. R., Sigmann, D. M., and Morel, F. M. M.: CO_2 effects on taxonomic composition and nutrient utilization in an Equatorial Pacific phytoplankton assemblage, Mar. Ecol.-Prog. Ser., 236, 37–43, 2002.

Tortell, P. D. and Morel, M. M.: Sources of inorganic carbon for phytoplankton in the Eastern Subtropical and Equatorial Pacific Ocean, Limnol. Oceanogr., 47, 1012–1022, 2002.

Tortell, P. D., Rau, G. H., and Morel, F. M. M.: Inorganic carbon acquisition in coastal Pacific phytoplankton communities, Limnol. Oceanogr., 45, 1485–1500, 2000.

Wu, H. Y. and Gao, K. S.: Ultraviolet radiation stimulated activity of extracellular carbonic anhydrase in the marine diatom *Skeletonema costatum*, Funct. Plant Biol., 36, 137–143, 2009.

Wu, Y., Gao, K., and Riebesell, U.: CO_2-induced seawater acidification affects physiological performance of the marine diatom *Phaeodactylum tricornutum*, Biogeosciences, 7, 2915–2923, doi:10.5194/bg-7-2915-2010, 2010.

BGD
9, 7197–7226, 2012

Xiong, F. S.: Evidence that UV-B tolerance of the photosynthetic apparatus in microalgae is related to the D1-turnover mediated repair cycle in vivo, J. Plant Physiol., 158, 285–294, 2001.

Xu, K., Gao, K., Villafañe, V. E., and Helbling, E. W.: Photosynthetic responses of Emiliania huxleyi to UV radiation and elevated temperature: roles of calcified coccoliths, Biogeosciences, 8, 1441–1452, doi:10.5194/bg-8-1441-2011, 2011.

BGD

9, 7197–7226, 2012

Table 1. Mean (±SD, n = 24) values of parameters of the seawater carbonate system under LC (ambient, 390 µatm CO_2) and HC (enriched, 1000 µatm CO_2) during the previous eight days of experiments. The superscripts represent significant difference between LC and HC.

PCO_2	pH_{NBS}	DIC (µmol kg^{-1})	HCO_3^- (µmol kg^{-1})	CO_3^{2-} (µmol kg^{-1})	CO_2 (µmol kg^{-1})	Total alkalinity (µmol kg^{-1})
LC	8.16±0.01^a	1903.3±47.66^a	1709.3±39.2^a	181.2±8.4^a	12.6^a	2171.0±57.8^a
HC	7.82±0.02^b	2127.3±75.3^b	1998.3±69.2^b	96.7±6.7^b	32.3^b	2246.4±84.0^a

BGD
9, 7197–7226, 2012

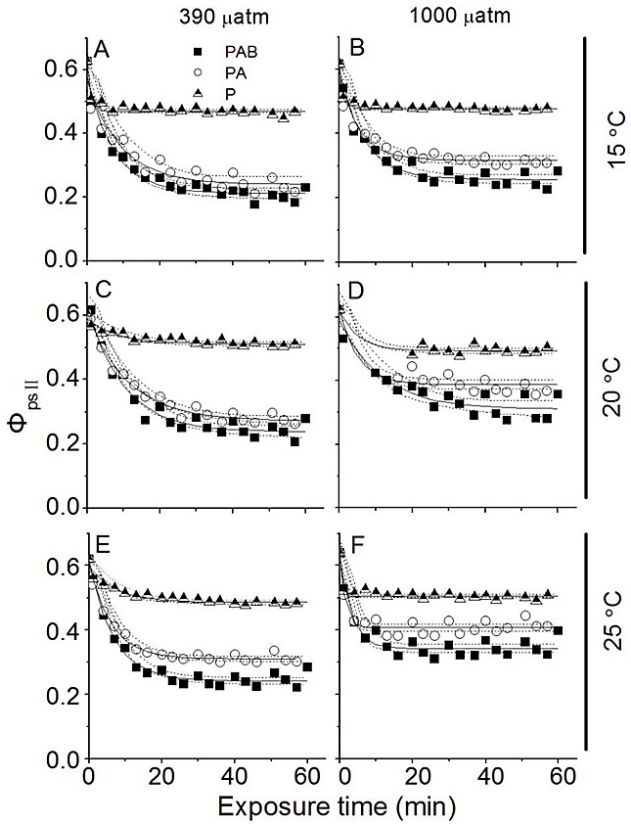

Fig. 1. Changes in effective photochemical quantum yield (Φ_{psII}) of *P. tricornutum* cells grown under ambient (390 µatm, LC) **(A, C** and **D)** and elevated CO_2 (1000 µatm, HC) partial pressures **(B, D** and **F)** when exposed to solar radiation for 60 min under three radiation treatments: PAB (irradiated above 295 nm, black squares), PA (irradiances above 320 nm, white circles) and P (irradiances above 395 nm, half solid triangles) at 15, 20 and 25 °C. Solid lines represent the best fit while the broken lines represent the 95 % confident limits.

BGD
9, 7197–7226, 2012

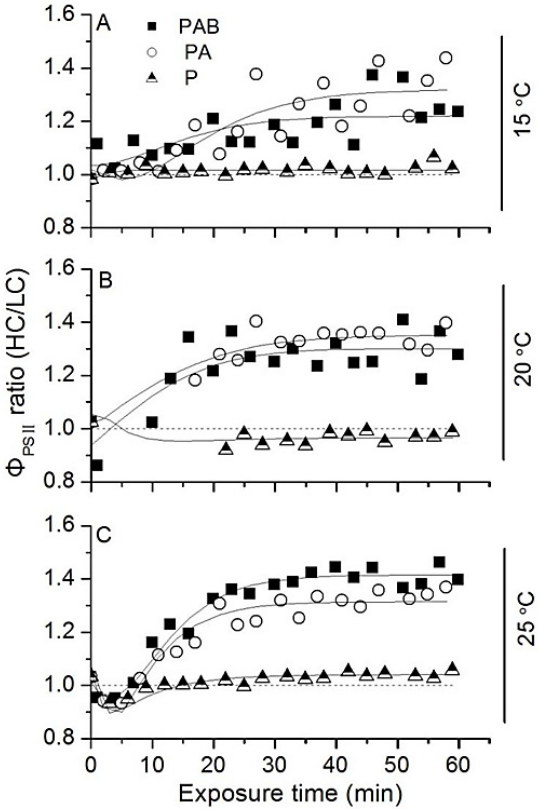

Fig. 2. Ratio of the HC to LC-grown cells' effective quantum yield (Φ_{psII}) in *P. tricornutum* exposed to the three radiation treatments PAB (irradiated above 295 nm, black squares), PA (irradiances above 320 nm, white circles) and P (irradiances above 395 nm, half solid triangles) at 15, 20 and 25 °C. Solid lines represent the best fit while the broken lines represent the value of 1.

BGD
9, 7197–7226, 2012

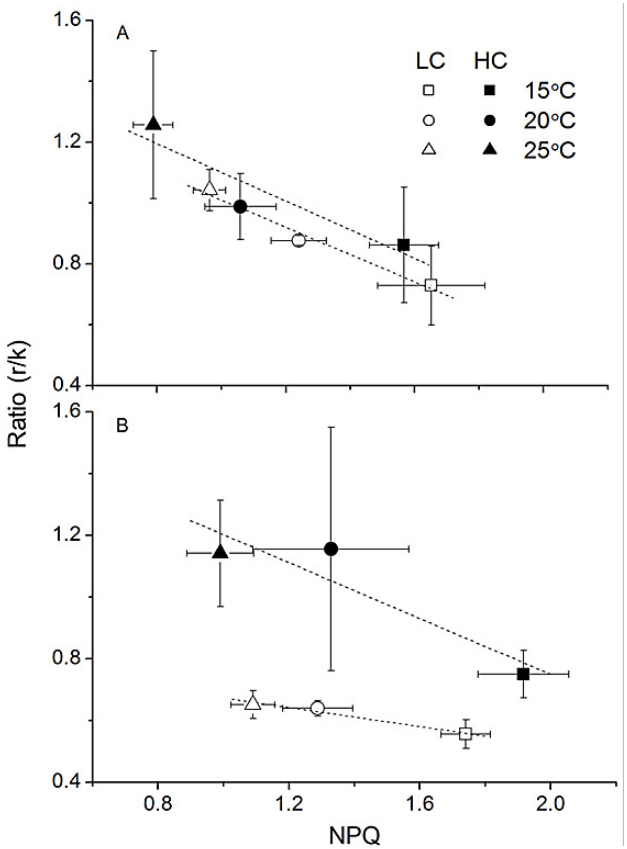

Fig. 3. Ratio of damage (k) to repair (r) as a function of non-photochemical quenching (NPQ) of *P. tricornutum* cells grown at ambient (LC, white symbols) and elevated CO_2 (HC, black symbols) concentrations when exposed to PAR+ UV-A **(A)** or PAR+UV-A+UV-B **(B)** at 15 (squares), 20 (circles) or 25 °C (triangles). The broken line represents the linear regression (**(A)**: R^2 = 0.86 (LC) and 0.98 (HC); **(B)**: R^2 = 0.85 (LC) and 0.97 (HC)).

BGD
9, 7197–7226, 2012

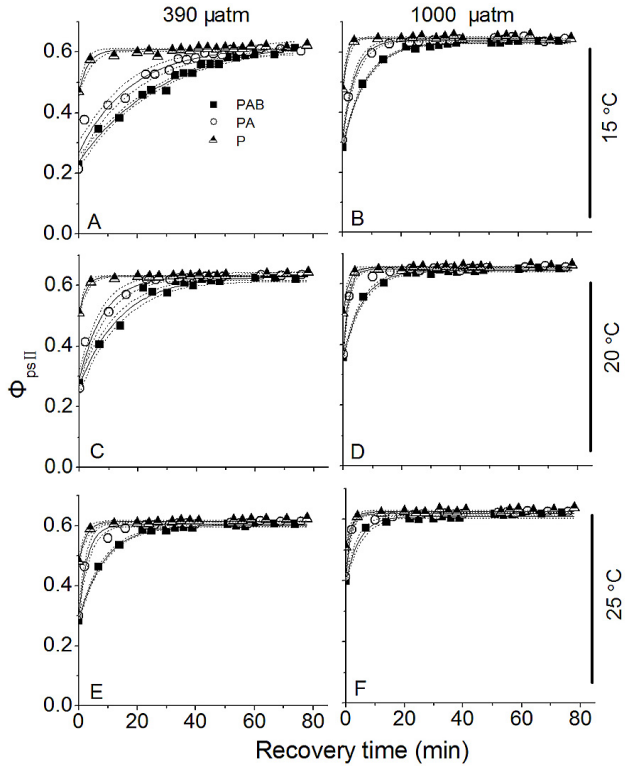

Fig. 4. Recovery of the effective photochemical quantum yield (Φ_{psII}) in the LC **(A, C** and **D)** and HC **(B, D** and **F)** grown cells of *P. tricornutum* after exposure to three radiation treatments: PAB (irradiated above 295 nm, black squares), PA (irradiances above 320 nm, white circles) and P (irradiances above 395 nm, half solid triangles) at 15, 20 and 25 °C. Solid lines represent the best fit while the broken lines represent the 95 % confident limits.

BGD
9, 7197–7226, 2012

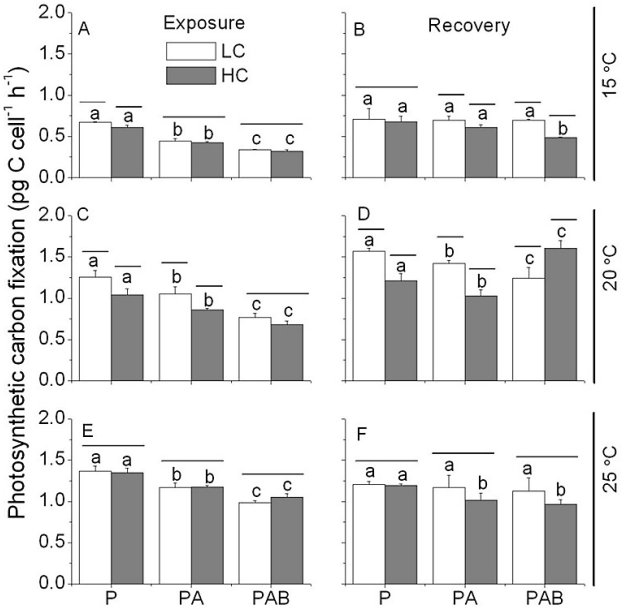

Fig. 5. Photosynthetic carbon fixation rates (in pg C cell^{-1} h^{-1}) in the LC (white bars) and HC (black bars) grown cells of *P. tricornutum* exposed to three radiation treatments: PAB (irradiated above 295 nm), PA (irradiances above 320 nm) and P (irradiances above 395 nm) at 15, 20 and 25 °C. **(A)**, **(C)** and **(E)** represents the carbon fixation rate during the 60 min exposure; while **(B)**, **(D)** and **(F)** represents that during the 60 min recovery period. The bars represent the means (n = 3) and the vertical lines on top are the standard deviation. Lines above the histogram bars indicate significant differences between LC and HC, and different letters indicate significant differences among the radiation treatments within the HC or LC-grown cells.

BGD
9, 7197–7226, 2012

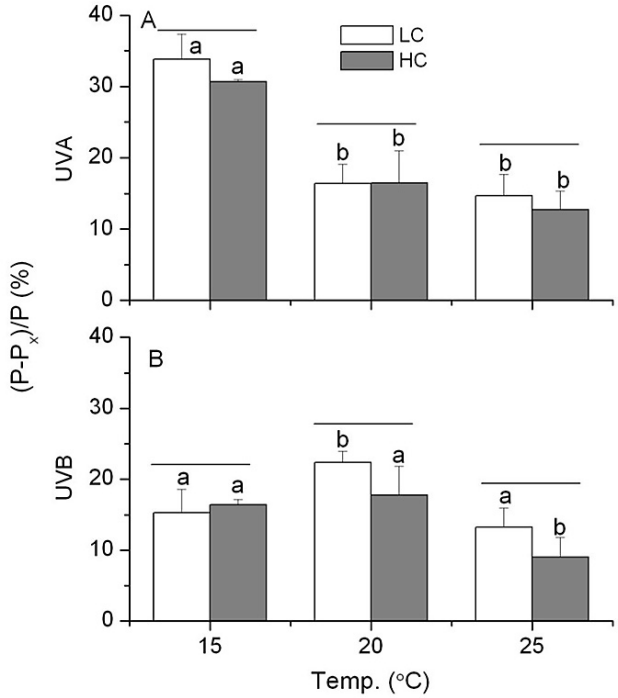

Fig. 6. Inhibition of photosynthetic carbon fixation of *P. tricornutum* grown at ambient (LC, white bars) and elevated CO_2 (HC, black bars) concentrations due to UV-A **(A)** or UV-B **(B)** exposed to three radiation treatments for 60 min at 15, 20 and 25 °C. The bars represent the means (n = 3) and the vertical lines on top are the standard deviation. Lines above the histogram bars indicate significant difference between LC and HC, and different letters indicate significant differences among the temperature treatments within the HC or LC-grown cells.

BGD
9, 7197–7226, 2012